Hybrid impedance control of a 3-DOF robotic arm used for rehabilitation treatment

Conference Paper · September 2010

DOI: 10.1109/COASE.2010.5584259 · Source: IEEE Xplore

2 authors:

Jingguo Wang
University of Macau

Yangmin Li
The Hong Kong Polytechnic University

6th annual IEEE Conference on Automation Science and Engineering
Marriott Eaton Centre Hotel
Toronto, Ontario, Canada, August 21-24, 2010

Hybrid Impedance Control of a 3-DOF Robotic Arm Used for Rehabilitation Treatment

Jingguo Wang and Yangmin Li*, *Senior Member, IEEE*

***Abstract*— A 3-DOF planar robotic arm is designed and used as a rehabilitation treatment tool for the survivor after suffering a stroke, aiming to assist them to recover upper-limb function. In order to strengthen the patient's arm, some forces are desired to be followed while the position trajectories should be tracked simultaneously, therefore hybrid impedance control (HIC) is proposed. Due to the redundancy for the planar motion, besides the main task, the secondary task is combined into the control scheme and the constraints of joint limits avoidance(JLA) are considered. Some typical trajectories are simulated for rehabilitation motion and a couple of simulations are made to study both the impedance control and hybrid impedance control strategies. The simulation results are compared and discussed and the tracking effectiveness of the proposed method is confirmed.**

I. INTRODUCTION

Robotic arms are widely used in rehabilitation therapy for the upper limb of stroke patients when the affected arm is trained in its initial phase. It will enable the patients to practice intensively with their upper paretic limb by applying some robot-assisted therapy [1]. Many 2-DOF robotic arms are applied for upper-limb planar motion in the rehabilitation treatment, like the MIT-MANUS [2], a robot is capable of executing desired trajectories in the cartesian space, but the wrist joint is usually neglected. The patient's wrist should be considered and practiced during the basic movement therapy and it will help to recover the whole upper-limb function. The movements of the patient's three joints(shoulder, elbow, wrist) are driven by mechanical active-assisted robot arm then the joints data can be recorded and followed up later.

This paper utilizes a 3-DOF robotic arm for rehabilitation therapy mainly aiming to assist survivors' affected arms after the stroke and to train their basic upper-limb function. The hybrid impedance control is applied not only to track the desired position trajectory but also to follow the force trajectory simultaneously [3]- [9].

This paper is organized as follows. In section 2 some related works are reviewed and discussed. In section 3, the compliant environment is modeled and the manipulator's dynamics is introduced in section 4. Hybrid impedance control method for redundant manipulator is carefully discussed in section 5. Finally, simulations are performed and their results are demonstrated in section 6 and the conclusion is given out in the last section.

This work was supported by Macao Science and Technology Development Fund under Grant 016/2008/A1 and the research committee of University of Macau under Grant UL016/08-Y2/EME/LYM01/FST.

The authors are with Department of Electromechanical Engineering, University of Macau, Macao SAR, China.

*Corresponding author Y.M. Li's E-mail: YMLi@umac.mo

II. SOME RELATED WORKS

Some related works can be found on studying the impedance control, which are highlighted in the follows.

The fundamental theory of impedance control is introduced by Hogan [5], when positions are commanded, and impedances are adjusted to obtain proper force response. It overcomes the problem of hybrid position-force control and emphasizes the importance of manipulator impedance. However, it is not able to follow a command force trajectory and ignore the distinction between force and position controlled subspace. A Hybrid Impedance Control(HIC)scheme is proposed as a combination of these two fundamental force control strategies in [4], and then a robust HIC method is proposed in [3] where the HIC is equivalent to tracking a desired acceleration trajectory and the computed torque technique is applied along with a PI feedback controller to make the system robust. With this control approach, the robustness of impedance control is maintained, and the interaction force can be controlled in the force controlled subspace. Adaptive control algorithms are applied to the tracking control of a target impedance reference trajectory in order to implement adaptive impedance control in [6]. An extended HIC scheme is presented which achieves an inertial decoupling of the motion and force controlled subspaces and internal motion control using a minimal parametrization of motion and force controlled subspaces and the null-motion component in [7]. An impedance controller is developed for manipulators carrying a rigid-body payload using an inner/outer loop feedback approach without needing any acceleration measurement [8]. Augmented Impedance Control(AIC) method is proposed in [10], which combines reduced-order impedance control with configuration control to achieve impedance control of the redundant manipulator. In [11], an Augmented Hybrid Impedance Control(AHIC) scheme is proposed for kinematically redundant manipulators combing redundancy resolution to achieve the regulation of the end-effector interaction with the environment and satisfy user defined additional constraints. An arm-like robot with five-bar-link drive mechanism has been designed and manufactured, the hybrid position/force control scheme incorporating fuzzy logic is applied for controlling the robot [16]. Haptic robots can emulate the soft interaction between patient and human therapist by providing a haptic virtual environment in treatment [17]. Some robotic devices are compared with respect to technical function, clinical applicability, and clinical outcomes in [18].

It is promising that robot-aided therapy will be adopted

978-1-4244-5449-5/10/$26.00 ©2010 IEEE

by clinics or families in future, which is safe, dependable, and task-specific treatment method enhancing upper limbs or lower limbs motor recovery in the stroke patients.

III. The compliant environment

In our desired application, the robotic devices are connected with the haptic virtual environment. The motion designed in the game(or virtual reality) should guide and assist the patient to perform some defined movement tasks, which need whole-joint coordination of shoulder, elbow and wrist.

As the environment is crucial to any force control strategy, the whole system in this paper can be regarded as a rigid manipulator in soft contact with a compliant environment [12] and the desired impedance is assumed to be a mass-spring-damper system. This kind of environment is usually modeled as a linear spring K, which is sometimes in parallel with a dashpot B_e. Both are considered to be known and constant, and a force control law is chosen accordingly when a rigid tool meets a compliant workpiece [4]. The environment consists of a damped, compliant surface with impedance $Z_e = Ms + B_e + K/s$ and is, by definition, capacitive.

When the robotic arm is in contact with the environment, force is generated between the end-effector and the environment. The amount of forces exerted by the robot to the environment depends on how much the end-effector position is physically constrained by the environment to reach its goal position [14]. Hence, the contact force can be regulated by appropriate control of the end-effector position. The hybrid impedance control used is to adjust the robot end-effector position in response to the sensed contact force in such a way that a target impedance relationship is satisfied.

IV. Manipulator dynamics in task space

The dynamics of the open-chain robot manipulator can be obtained using energy-based Lagrange method, which is based on the principle of virtual work function. $L = T - V$, where the *Lagrangian*, *L*, is defined as the difference between the kinetic energy *T* and the potential energy *V* of the whole system. For manipulator's compliant motion, control tasks are always described in task space. Then in the absence of friction, the dynamics of the manipulator can be written as:

$$M(X)\ddot{X} + C(X,\dot{X})\dot{X} + G(X) = F - F_e \qquad (1)$$

where $M(X)$ is the nonsingular symmetric inertia matrix, $C(X,\dot{X})$ is the vector that implicitly includes centrifugal, coriolis and viscous friction, $G(X)$ is the gravity terms, F is the input control force and F_e is the interaction force between the manipulator and the environment.

The vector of generalized input force F is related to the vector of input joint torque τ by the Jacobian matrix J,

$$\tau = J^T(q)F \qquad (2)$$

V. Hybrid impedance control for redundant manipulator

A. Hybrid impedance control

The impedance control proposed in [5] has the form as follows:

$$M_d(\ddot{x} - \ddot{x}_d) + B_d(\dot{x} - \dot{x}_d) + K_d(x - x_d) = -F_e \qquad (3)$$

where M_d, B_d and $K_d \in R^{m\times m}$ are positive-definite matrices representing inertia, damping and stiffness respectively, which are usually chosen to be diagonal, rendering the system decoupled, and F_e is the environmental reaction forces.

As also discussed in previous section, impedance control makes the robot behave as a mass-spring-dashpot system, so the force of interaction due to uncertainty on the location of the point of contact and environments structural properties is regulated [3]. However the impedance control is only a position control scheme, with adjustments made to control the contact forces, and it has no any attempt to follow a command force trajectory. Therefore, the hybrid impedance control proposed in [4] is defined as follows:

$$M_d(\ddot{x}-S\ddot{x}_d)+B_d(\dot{x}-S\dot{x}_d)+K_dS(x-x_d)-(I-S)F_d = -F_e \qquad (4)$$

Here the task space is divided into orthogonal position and force controlled subspaces using the selection matrix S. S is diagonal with ones and zeros on the diagonal while ones on the diagonal relate to position-controlled subspaces and zeros relate to the force-controlled subspaces. F_d is the desired force. The desired equation of motion in the position-controlled subspaces is identical to (5).

$$M_d\ddot{e}_p + B_d\dot{e}_p + K_de_p = -F_e \qquad (5)$$

where e_p is the position tracking error and $e_p = X - X_d$.

In the force-controlled subspace, the desired impedance is defined by

$$M_d\ddot{x} + B_d\dot{x} - F_d = -F_e \qquad (6)$$

B. Redundancy resolution at the acceleration level

For a redundant manipulator, a nonempty null space exists, which allows the user to analytically apply the redundancies of the system in a strategic manner that will improve performance while modifying the null-space will lead to an infinite number of solutions to the original problem. Therefore, the redundancy will make the robot achieve many advantages such as avoidance of obstacles, joint limits and the singular configurations, or minimization of impacting forces between the end-effector of a manipulator and an environment [9]. The joint space dynamics can be transformed into the task space and a set of minimal parameters in the null space by defining the weighted inner product in joint space [7], and a decoupled impedance controller can be applied to control the motion of the end-effector as well as the internal motion.

Based on the HIC idea, the spaces are split into the main task X and additional task Z and their equations of motions have similar forms as (4). The trajectories of accelerations $\ddot{X}$

of main tasks and $\ddot{Z}$ of additional tasks have the following forms:

$$\begin{aligned}\ddot{X} &= S_x\ddot{X}_d - M_{xd}^{-1}[B_{xd}(\dot{X} - S_x\dot{X}_d) + K_{xd}S_x(X - X_d) \\ &-(I - S_x)F_{xd} + F_{xe}]\end{aligned} \tag{7}$$

$$\begin{aligned}\ddot{Z} &= S_z\ddot{Z}_d - M_{zd}^{-1}[B_{zd}(\dot{Z} - S_z\dot{Z}_d) + K_{zd}S_z(Z - Z_d) \\ &-(I - S_z)F_{zd} + F_{ze}]\end{aligned} \tag{8}$$

where S_x and S_z are diagonal elements of the selection matrix S, $S = diag(S_x, S_z)$ and similarly, $M_d = diag(M_{xd}, M_{zd})$, $K_d = diag(K_{xd}, K_{zd})$, $F_d = diag(F_{xd}, F_{zd})$ and $F_e = diag(F_{xe}, F_{ze})$.

For compliant motion, dynamic control of redundant manipulators in task space requires the computation of joint accelerations. Hence, redundancy resolution should be performed at the acceleration level. The differential kinematics equations have the forms as follows:

$$\begin{aligned}\dot{X} &= J_e(q)\dot{q} \\ \ddot{X} &= \dot{J}_e(q)\dot{q} + J_e(q)\ddot{q}\end{aligned} \tag{9}$$

where $J_e(q)$ is the Jacobian of the end-effector.

Then the joint acceleration can be solved by the pseudo inverse of the Jacobian matrix $J_e^{\dagger}$:

$$\ddot{q} = J_e^{\dagger}(\ddot{X} - \dot{J}_e\dot{q}) \tag{10}$$

Similar to the pseudo-inverse solution, the following weighted damped least-squares solution [11] can be obtained:

$$\begin{aligned}\ddot{q} &= [J_e^TW_eJ_e + J_c^TW_cJ_c + W_v]^{-1}[J_e^TW_e(\ddot{X} - \dot{J}_e\dot{q}) \\ &+J_c^TW_c(\ddot{Z} - \dot{J}_c\dot{q})]\end{aligned} \tag{11}$$

which minimizes the following cost function:

$$L = \ddot{E}_e^TW_e\ddot{E}_e + \ddot{E}_c^TW_c\ddot{E}_c + \ddot{q}^TW_v\ddot{q} \tag{12}$$

where W_e, W_c and W_v are diagonal positive-definite weighting matrices that assign priority between the main, additional and singularity robustness tasks. The velocity errors of the main and additional tasks are $\ddot{E}_e = \ddot{X}_d - (\ddot{X} - \dot{J}_e\dot{q})$ and $\ddot{E}_c = \ddot{Z}_d - (\ddot{Z} - \dot{J}_c\dot{q})$

C. Impedance control law

In the absence of friction and disturbances, the joint-space dynamic equation of rigid manipulator's motion is described by:

$$M(q)\ddot{q} + C(q,\dot{q})\dot{q} + G(q) = \tau + J_e^TF_e \tag{13}$$

The proposed control scheme is shown in Fig. 1. The inner and outer loop control strategy can be combined to achieve the closed-loop dynamics [11]. The outer loop outputs the acceleration trajectories reflecting the desired impedance in the position-controlled subspaces as pointed in (7) and (8), and the desired force in the force-controlled subspaces of the main and additional tasks as pointed in (6). The inner-loop control is to select an input to the actuators which makes the end-effector track the desired trajectories generated by the outer loop. The input torque of the manipulator dynamics is defined as:

$$\tau = M(q)\ddot{q} + C(q,\dot{q})\dot{q} + G(q) - J_e^TF_e \tag{14}$$

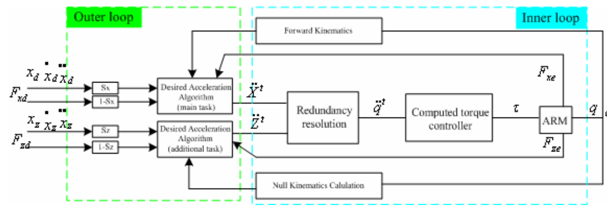

Fig. 1. The hybrid impedance control scheme

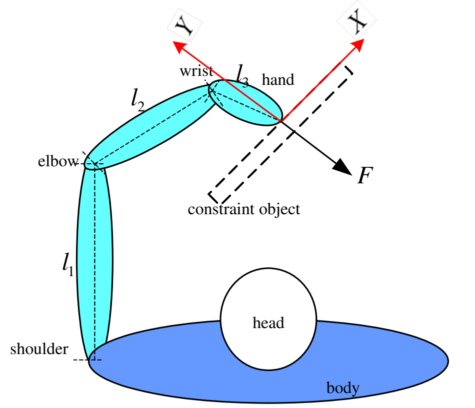

Fig. 2. 3-DOF planar robotic arm for rehabilitation therapy

D. Joint limit avoidance

In addition to the primary task, the secondary task is to minimize a desired cost function. Here the kinematic constraint function considered is the joint limit avoidance defined as [9]

$$\Phi(q) = \frac{1}{n}\sum_{i=1}^{n}\left(\frac{q_i - \bar{q}_i}{q_{iM} - q_{im}}\right)^2 \tag{15}$$

where $q_{iM}(q_{im})$ denotes the maximum(minimum) limit for q_i and $\bar{q}_i$ the middle value of the joint range, and thus the redundancy resolution problem is to define a joint trajectory which optimizes (15) subject to the end-effector position.

VI. Cases study

The planar motion aims to train the stroke patients recovering their moving ability as the first step of the rehabilitation work, and a simplified model is to show its application purpose in Fig. 2. The hybrid impedance control is considered here not only to track position trajectory in one direction (like X) but also to track force trajectory in another direction (like Y). In order to compare the effectiveness of the proposed control method, simulations of the impedance control in two directions are also given out.

A. Initial parameters

The length parameters are $l_1 = 0.25m$, $l_2 = 0.25m$, $l_3 = 0.1m$ and the masses of links are $m_1 = 3kg$, $m_2 = 2kg$, $m_3 = 1kg$. Their inertias about axis z have the following values: $I_{z1} = 0.0625kg.m^2$, $I_{z2} = 0.0417kg.m^2$, $I_{z3} = 0.0033kg.m^2$.

Due to the planar manipulator is designed almost based on the human actual arm, three joints limits are defined as: $-80deg \leq q_1 \leq 80deg$ of shoulder joint, $-120deg \leq q_2 \leq 0deg$ of elbow joint and $-80deg \leq q_3 \leq 30deg$ of wrist joint.

The Jacobian matrix of the manipulator is given out as follows:

$J_e(1,1) = -l_1 * s1 - l_2 * s12 - l_3 * s123;$
$J_e(2,1) = l_1 * c1 + l_2 * c12 + l_3 * c123;$
$J_e(1,2) = -l_2 * s12 - l_3 * s123;$
$J_e(2,2) = l_2 * c12 + l_3 * c123;$
$J_e(1,3) = -l_3 * s123;$
$J_e(2,3) = l_3 * c123;$

The symmetric positive definite inertia matrix $M(q)$ can be given by: $M(1,1) = 0.4381 + 0.025(10c2 + c3 + c23); M(1,2) = 0.1413 + 0.0125(10c2 + 2c3 + c23); M(1,3) = 0.0058 + 0.0125(c3 + c23); M(2,2) = 0.1415 + 0.025c3; M(2,3) = 0.0058 + 0.0125c3; M(3,3) = 0.0058$.

The matrix of Centrifugal and Coriolis forces $C(q)$ will have the following form: $C(1,1) = -0.0125(10d2s2 + d3s3 + (d2 + d3)s23); C(1,2) = 0.0125(10d1s2 - d3s3 + d1s23); C(1,3) = 0.0125d2s3; C(2,1) = -0.0125(10(d1 + d2)s2 + d3s3 + (d1 + d2 + d3)s23); C(2,2) = -0.0125d3s3; C(2,3) = 0.0125(d1 + d2)s3; C(3,1) = -0.0125(d1 + d2 + d3)(s3 + s23); C(3,2) = -0.0125(d1 + d2 + d3)s3; C(3,3) = 0$.

where $s1 = sin(q_1); c1 = cos(q_1); s12 = sin(q_1 + q_2); d1 = \dot{q}_1$, and so on.

The weighting diagonal elements in the weighting matrices of the redundancy resolution have the values as $we = 10; wc = 100; wv = 20$.

Other parameters' values for simulation are: $M_d = 5; B_d = 200; K_d = 3000; K_e = diag(10000, 10000)$.

B. Simulations of impedance control

When we set $S_x = diag(1,1)$, the impedances in two directions are position-controlled as pointed in the previous sections. The desired trajectory is chosen as

$$\begin{bmatrix} X_d(t) \\ Y_d(t) \end{bmatrix} = \begin{bmatrix} 0.3250 + 0.1cos(\pi t/2) \\ 0.1799 - 0.05cos(\pi t/2) \end{bmatrix}.$$

The reason for choosing this trajectory is to imitate the patients' non-smooth moving path. The simulation time is set to $4s$, then it is a cycle trajectory with the forward path and back repeated path.

The initial posture of the manipulator is set with joint initial values $q_0 = \begin{bmatrix} pi/3 & -pi/3 & -pi/3 \end{bmatrix}$ corresponding to the initial position $p = \begin{bmatrix} 0.4250 & 0.1299 \end{bmatrix}^T$ and all the joints initial velocities are $\dot{q}_0 = \begin{bmatrix} 0 & 0 & 0 \end{bmatrix}$ at the very beginning.

In the first simulation, the constraint of joint limit avoidance(JLA) is combined into the impedance control, and the simulation results are shown in Fig. 3. It is easy to know all the joints did not exceed their limits during the whole simulation from Fig. 3(b). The tracking position errors are shown in Fig. 3(a). The trajectory is well followed and then repeated as shown in Fig. 3(c) and Fig. 3(d).

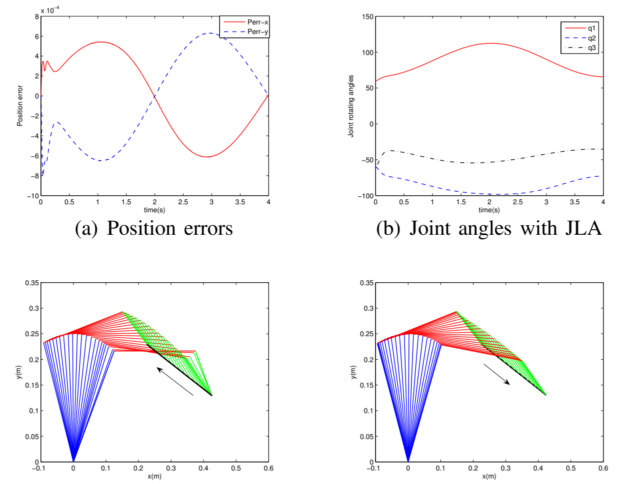

(a) Position errors (b) Joint angles with JLA

(c) The forward motion trajectory (d) The backward motion trajectory

Fig. 3. Simulation results of impedance control considering the JLA constraint

In the second simulation, the constraint of JLA is not considered, and the simulation results are shown in Fig. 4. It can be found that the third joint (waist joint) exceeds its lower limit ($q_{3min} = -80deg$) from Fig. 4(b). The tracking position error is shown in Fig. 4(a) and the forward and backward moving trajectories are shown in Fig. 4(c) and Fig. 4(d) respectively. Compared with the first simulation, the first joint has less moving range but the third joint has large one.

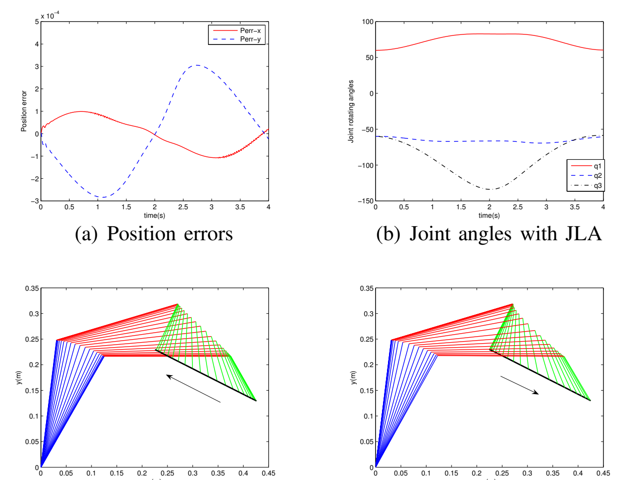

(a) Position errors (b) Joint angles with JLA

(c) The forward motion trajectory (d) The backward motion trajectory

Fig. 4. Simulation results of impedance control not considering the JLA constraint

C. Simulations of hybrid impedance control

When the selection matrix is set to $S_x = diag(0, 1)$, it becomes the hybrid impedance control, which is not only to track the position trajectory in X direction but also to track the force trajectory in Y direction.

The desired trajectory is chosen as

$$\begin{bmatrix} X_d(t) \\ F_d(t) \end{bmatrix} = \begin{bmatrix} 0.3250 + 0.1cos(\pi t/2) \\ -30 + 5sin(\pi t/2) \end{bmatrix}.$$

An virtual environment constraint has been simulated as an elastic compliant system and the interaction force between the robot and the constraint K_e can be known by the following force equation:

$$F_e = K_e(X_e - x) \quad (16)$$

The first simulation is to track both $X_d(t)$ in X direction and $F_d(t)$ in Y direction and the constraint of JLA is combined into it. The simulation results can be seen in Fig. 5. It can be observed that the desired force has been followed well from Fig. 5(a) while all the joints do not exceed their limits in Fig. 5(b). The motion trajectories in the forward and backward directions are shown in Fig. 5(c) and Fig. 5(d).

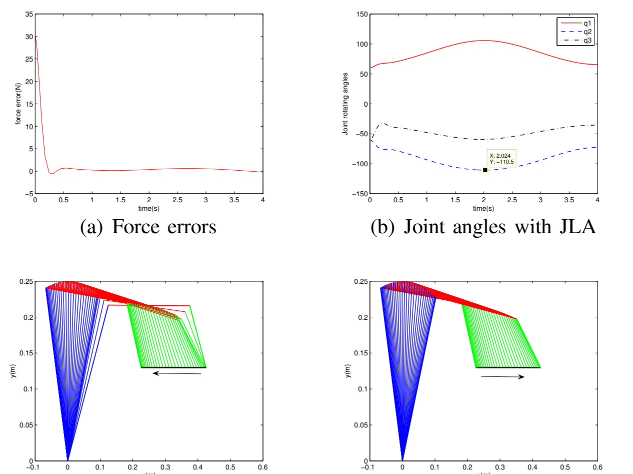

(a) Force errors (b) Joint angles with JLA

(c) The forward motion trajectory (d) The backward motion trajectory

Fig. 5. Simulation results of hybrid impedance control considering the JLA constraint

The second simulation is also to track both $X_d(t)$ in X direction and $F_d(t)$ in Y direction but the constraint of JLA is not considered. The simulation results can be seen in Fig. 6. It is easily found that the third joint exceeds its low limit from Fig. 6(b). Although the desired force is also followed well in this simulation from Fig. 6(a), it does not have as good performance as the first simulation. The motion trajectories in the forward and backward directions are shown in Fig. 6(c) and Fig. 6(d).

VII. Discussion

With respect to the development of robots for rehabilitation purpose, we can design various types of robots according to different design criteria. The safety issue is the most important one, the second one needs to be considered is lower in cost and easy to be used by patients. Introducing computer techniques in terms of virtual reality and computer games into the robotic therapy system, we can realize to recover the function of limbs by playing computer games, patients will not be boring at doing exercises.

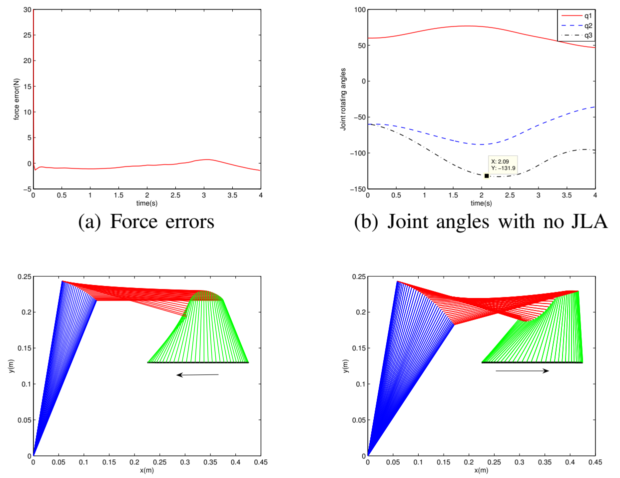

(a) Force errors (b) Joint angles with no JLA

(c) The forward motion trajectory (d) The backward motion trajectory

Fig. 6. Simulation results of hybrid impedance control not considering the JLA constraint

With respect to effective control of robotic arm, more control methods can be exploited and compared in order to find the best one. In most force control schemes, the dynamics model of the manipulator always can not be known exactly for two reasons, one is the uncertainties in modeling due to limitations in measurement techniques and the other is incomplete dynamic model. Also, there is unmodeled dynamic behavior presented at high frequencies. Both parametric uncertainties and external disturbances affect the stability and the performance of the system.

The issues of uncertainties and robustness will be investigated in future. Different strategies have been applied to solve this problem. A novel robust impedance control of robot manipulators in the presence of both parametric uncertainties and external disturbances [13] is proposed by using variable structure model reaching control. To improve the impedance controller robustness, the neural network technique is applied to compensate for the uncertainties in the robot model [14]. The computed torque technique and a PI control law are used to reduce the influence of model uncertainties [3]. An adaptive impedance control technique is utilized in [15]. Since performance of impedance controller for robot force tracking is affected by the uncertainties in the robot model and environment stiffness, the robustness issues should be considered in control schemes.

VIII. Conclusion

In order to practice the upper-limb of a patient after the stroke, a 3-DOF planar robotic arm is designed to do the rehabilitation treatment, which imitates the actual human arm with shoulder, elbow and wrist joint while the wrist joint is always be neglected in previous research works. Then hybrid impedance control method is applied to track both the position and the force trajectory. The control space is split into position-controlled subspace and force-controlled subspace by modifying the selection matrix S. The hybrid impedance control laws are given out. Simulations are made for both the impedance control and hybrid impedance control, and their results show the proposed control method can track both the position and force trajectory well.

In our future work, a real 3-DOF manipulator will be designed in details and manufactured in our laboratory. Based on our previous works on theoretical analysis and control simulations, we have a great confidence to build up the robot with haptic device to interact with computer or therapist, our goal is to let patients to train the arms with amusement. The robotic prototype will be tested on real stroke patients to confirm its effectiveness and find its shortcomings at the same time, an improvement on the design will be made after tests, and a satisfied robotic therapy device is fabricated and expected finally.

REFERENCES

[1] G. Kwakkel, B. J. Kollen and H. I. Krebs, “Effects of robot-assisted therapy on upper limb recovery after stroke: a systematic review,” *Neurorehabil Neural Repair*, Vol. 22(2), pp. 111–121, 2008.

[2] D. Formica, L. Zollo, and E. Guglielmelli, “Torque-dependent compliance control in the joint space of an operational robotic machine for motor therapy”, *IEEE Int. Conf. on Rehabilitation Robotics*, Chicago, IL, USA, 2005, pp. 341–344.

[3] G. J. Liu and A. A. Goldenberg, “Robust hybrid impedance control of robot manipulators”, *IEEE Int. Conf. on Robotics and Automation*, California, USA, 1991, pp. 287–292.

[4] R. Anderson and M. W. Spong, “Hybrid impedance control of robotic manipulators”, *IEEE Journal of Robotics and Automation*, Vol. 4(5), pp. 549–556, 1988.

[5] N. Hogan, “Impedance control: An approach to manipulation, part I-theory”, *ASME J. Dyn. Syst., Meas., Control*, Vol. 107, pp. 1–7, 1985.

[6] W. S. Lu and Q. H. Meng, “Impedance control with adaptation for robotic manipulators”, *IEEE Trans. on Robotics and Automation*, Vol. 7(3), pp. 408–415, 1991.

[7] Y. Oh, W. K. Chung, Y. Youm, and I. H. Suh, “Motion/force decomposition of redundant manipulators and its application to hybrid impedance control”, *IEEE Int. Conf. on Robotics and Automation*, Leuven, Belgium, 1998, pp. 1441–1446.

[8] F. Aghili, “Impedance control of manipulators carrying a heavy payload”, *IEEE Int. Conf. on Robotics and Automation*, St. Louis, USA, 2009, pp. 3410–3415.

[9] J.-G. Wang and Y.M. Li, “Impedance control of a spatial redundant manipulator used for relaxing muscle fatigue,” *IEEE Int. Conf. on Mechatronics and Automation*, Changchun, Jilin, China, 2009, pp.2799-2804.

[10] W. S. Newman and M. E. Dohring, “Augmented impedance control: an approach to compliant control of kinematically redundant manipulators”, *IEEE Int. Conf. Robotics and Automation*, California, USA, 1991, pp. 30–35.

[11] F. Shadpey, R. V. Patel, C. Balafoutis, and C. Tessier, “Compliant motion control and redundancy resolution for kinematically redundant manipulators”, *American Control Conference*, Seattle, WA, 1995, pp. 392–396.

[12] J. De Schutter and H. Van Brussel, “Compliant robot motion II. A control approach based on external control loops,” *Int. J. Robot. Res.*, Vol. 7(4), pp. 18–33, 1988.

[13] S. P.Chan, B. Yao, W. B. Gao, and M. Cheng, “Robust impedance control of robot manipulators,” *Int. J. Robotics and Automation*, Vol. 6(4), pp. 220–227, 1991.

[14] S. Jung and T.C. Hsia, “On neural network application to robust impedance control of robot maniplulators,” *IEEE Int. Conf. Robotics and Automation*, Nagoya, Japan, 1995, pp. 869–874.

[15] R. Colbaugh, H. Seraji, and K. Glass, “Direct adaptive impedance control of robot manipulators”, *J. Robotic Systems*, Vol. 10, pp. 217–248, 1993.

[16] M. S. Ju, C. C. K. Lin, D. H. Lin, I. S. Hwang, and S. M. Chen, “A rehabilitation robot with force-position hybrid fuzzy controller: hybrid fuzzy control of rehabilitation robot”, IEEE Trans. on Neural Systems and Rehabilitation Engineering, 13(3), pp. 349-358, 2005.

[17] P. Morasso, M. Casadio, V. Sanguineti, V. Squeri, and E. Vergaro, “Robot therapy: the importance of haptic interaction”, Proc. IEEE Virtual Rehabilitation, Venice, Sept. 27-29, 2007, pp. 70-77.

[18] R. Riener, “Robot-aided rehabilitation of neural function in the upper extremities”, Acta Neurochir Suppl, 97(1): 465-471, 2007.